



Bergische Universität Wuppertal

Fakultät für Mathematik und Naturwissenschaften

Institute of Mathematical Modelling, Analysis and Computational
Mathematics (IMACM)

Preprint BUW-IMACM 24/01

Julia Ackermann, Matthias Ehrhardt, Thomas Kruse and Antoine Tordeux

**Stabilisation of stochastic single-file dynamics
using port-Hamiltonian systems**

January 30, 2024

<http://www.imacm.uni-wuppertal.de>

Stabilisation of stochastic single-file dynamics using port-Hamiltonian systems

Julia Ackermann,* Matthias Ehrhardt,* Thomas Kruse,*
Antoine Tordeux**

* *Applied and Computational Mathematics, IMACM, University of Wuppertal, Germany*

** *Traffic Safety and Reliability, University of Wuppertal, Germany*
e-mail: {jackermann/ehrhhardt/tkruse/tordeux}@uni-wuppertal.de

Abstract: This study revisits a recently proposed symmetric port-Hamiltonian single-file model in one dimension. The uniform streaming solutions are stable in the deterministic model. However, the introduction of white noise into the dynamics causes the model to exhibit divergence. In response, we introduce a control term in a port-Hamiltonian framework. Our results show that this control term effectively stabilises the dynamics even in the presence of noise, providing valuable insights for the control of road traffic flows.

Keywords: Port-Hamiltonian systems, Multi-agent systems, Asymptotic stabilisation, Modelling and control of road traffic flows

2000 MSC: 76A30, 82C22, 60H10, 37H30

1. INTRODUCTION

The stability of single-file dynamics is of great interest in traffic engineering. Pioneering work by Reuschel, Pipes, and others (Reuschel, 1950; Pipes, 1953; Kometani and Sasaki, 1958; Chandler et al., 1958) have shown that single file traffic flow can present stability problems. Although the problem dates back to the 1950s and early 1960s and has been actively researched since then, see the review of Wilson and Ward (2011), it is still relevant today. Even current adaptive cruise control (ACC) systems exhibit unstable dynamics in experiments, cf. the results in Gunter et al. (2020); Makridis et al. (2021); Ciuffo et al. (2021).

In fact, many factors can perturb the stability of single-file uniform streaming. It is a well-known fact that lag and delay in the dynamics can lead to *linear instability* of the uniform equilibrium solution, see Gasser et al. (2004); Orosz et al. (2010); Tordeux et al. (2012, 2018). More recent approaches show that additive stochastic noise can also perturb single-file dynamics, even for stable deterministic systems, cf. Treiber and Helbing (2009); Tordeux and Schadschneider (2016); Treiber and Kesting (2017); Friesen et al. (2021); Ehrhardt et al. (2024).

Port-Hamiltonian systems (pHS) have recently emerged as a modelling framework for nonlinear physical systems, cf. van der Schaft and Jeltsema (2014). Unlike conservative Hamiltonian systems, pHS integrate control and external forcing into the dynamics through input and output ports. PHS can represent systems from diverse physical domains such as thermodynamics, electromechanics, electromagnetics, fluid mechanics and hydrodynamics, cf. Rashad et al. (2020). The functional structure of pHS, which extends the Hamiltonian framework with dissipation, input

and output ports, serves as a meaningful representation for a wide range of physical systems.

Recent research shows that pHS provide valuable modelling techniques for multi-agent systems, including multi-input multi-output (MIMO) systems (Sharf and Zelazo, 2019), swarm behaviour (Matei et al., 2019), interacting particle systems (Jacob and Totzeck (2023)), pedestrian dynamics (Tordeux and Totzeck, 2023), or autonomous vehicles and adaptive cruise control systems (Knorn et al., 2014; Dai and Koutsoukos, 2020). These micro-level agent-based models are constructed using finite-dimensional pHS. In addition, macroscopic traffic flow models (Bansal et al., 2021) and more general fluid dynamics models (Rashad et al., 2021a,b) use infinite-dimensional pHS.

In this paper, we first recall a symmetric port-Hamiltonian single-file model recently introduced to describe collection motions in one dimension, see Ehrhardt et al. (2024). Interestingly, the uniform solutions are stable for the deterministic model. However, the introduction of white noise in the dynamics causes the model to diverge. We show that the introduction of a control term - the input port in the port-Hamiltonian formulation - allows the dynamics to be stabilised even in the presence of noise.

The paper is structured as follows. In the next section, we introduce the port-Hamiltonian single-file model, elucidating its intricacies, and additionally, we expound upon its extension with the inclusion of the input control term. The analysis of the long-term behavior of the models, coupled with an exploration of their behavior as the number of agents N approaches infinity, is presented in Section 3. Some simulation results with a line of 10 agents are shown in Section 4. Section 5 is dedicated to discussions that not only encapsulate the key findings but also propose potential avenues for further extensions of the model.

2. PORT-HAMILTONIAN SINGLE-FILE MODELS

Let us first start with the notations and the definitions of the models we are considering.

Notations. We consider $N \in \{3, 4, \dots\}$ agents on a segment of length L with periodic boundaries. We denote

$$q(t) = (q_n(t))_{n=1}^N \in \mathbb{R}^N, \quad t \in [0, \infty),$$

the positions of the agents and

$$p(t) = (p_n(t))_{n=1}^N \in \mathbb{R}^N, \quad t \in [0, \infty),$$

are the velocities of the agents at time t . We assume that the positions $q(t)$ and the velocities $p(t)$ of the N agents are known at time $t = 0$,

$$p(0) = p|_{t=0} = \mathbf{p} \in \mathbb{R}^N, \quad q(0) = q|_{t=0} = \mathbf{q} \in \mathbb{R}^N,$$

and that the positions of the agents are initially ordered by their indices, i.e.,

$$0 \leq q_1(0) \leq q_2(0) \leq \dots \leq q_N(0) \leq L. \quad (1)$$

Furthermore, in the following we consistently use the index $n + 1$ to represent the nearest neighbour on the right and $n - 1$ for the nearest neighbour on the left. The right neighbour of the N -th agent is the first agent, i.e., $n + 1 = 1$ when $n = N$. Conversely, the left neighbour of the first agent is the N -th agent, i.e., $n - 1 = N$ if $n = 1$.

The distances to the right neighbours (see Fig. 1)

$$Q(t) = (Q_n(t))_{n=1}^N \in \mathbb{R}^N, \quad t \in [0, \infty),$$

are given by

$$\begin{cases} Q_n(t) = q_{n+1}(t) - q_n(t), & n \in \{1, \dots, N-1\}, \\ Q_N(t) = L + q_1(t) - q_N(t). \end{cases} \quad (2)$$

The distance to the left is Q_n for the first agent and Q_{n-1} for the n -th agent, $n \in \{2, \dots, N\}$. The index order of the agents at time zero makes the initial distance positive

$$Q(0) = Q|_{t=0} := \mathfrak{Q} \in [0, \infty)^N.$$

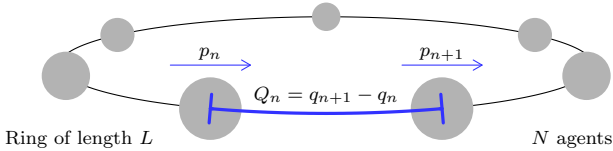


Fig. 1. Illustration of the single-file motion system with periodic boundary conditions. Here, q_n represents the curvilinear position, $Q_n = q_{n+1} - q_n$ is the distance to the right neighbour and p_n denotes the velocity of the n -th vehicle.

2.1 Initial stochastic motion model

First, we introduce a probability space $(\Omega, \mathcal{F}, \mathbb{P})$ on which there exists an N -dimensional standard Brownian motion

$$W = (W_n)_{n=1}^N : [0, \infty) \times \Omega \rightarrow \mathbb{R}^N.$$

For the n -th agent at time $t \in [0, \infty)$, the model reads

$$\begin{cases} dQ_n(t) = (p_{n+1}(t) - p_n(t)) dt, \\ dp_n(t) = (U'(Q_n(t)) - U'(Q_{n-1}(t))) dt \\ \quad + \beta(p_{n+1}(t) - 2p_n(t) + p_{n-1}(t)) dt + \sigma dW_n(t), \\ Q(0) = \mathfrak{Q}, \quad p(0) = \mathbf{p}, \end{cases} \quad (3)$$

where $\beta \in (0, \infty)$ is the dissipation rate, $\sigma \in \mathbb{R}$ is the noise volatility, and U' is the derivative of a convex potential

$U \in C^1(\mathbb{R}, [0, \infty))$. In the following, we use the quadratic functional

$$U(x) = \frac{1}{2}(\alpha x)^2, \quad x \in \mathbb{R}, \quad \alpha \in (0, \infty). \quad (4)$$

Remark 1. The ensemble's mean velocity

$$\bar{p}(t) = \frac{1}{N} \sum_{n=1}^N p_n(t), \quad t \in [0, \infty), \quad (5)$$

is a Brownian motion with variance σ^2/N for any potential function U . In fact, thanks to the telescopic form of the model (3) and the periodic boundaries, we have

$$d\bar{p}(t) = \frac{1}{N} \sum_{n=1}^N dp_n(t) = \frac{\sigma}{N} \sum_{n=1}^N dW_n(t), \quad t \in [0, \infty).$$

In addition, the ensemble's mean velocity (5) is conserved for the deterministic system with $\sigma = 0$.

2.2 Extended stochastic motion model

The motion model (3) is symmetric and there is no inherent preference or favoured direction of motion. In the following model we introduce a *relaxation process* to a desired velocity $u \in \mathbb{R}$ with relaxation rate $\gamma \in [0, \infty)$. The extended motion model reads for the n -th agent at time $t \in [0, \infty)$

$$\begin{cases} dQ_n(t) = (p_{n+1}(t) - p_n(t)) dt, \\ dp_n(t) = (U'(Q_n(t)) - U'(Q_{n-1}(t))) dt \\ \quad + \beta(p_{n+1}(t) - 2p_n(t) + p_{n-1}(t)) dt \\ \quad + \gamma(u - p_n(t)) dt + \sigma dW_n(t), \\ Q(0) = \mathfrak{Q}, \quad p(0) = \mathbf{p}. \end{cases} \quad (6)$$

Note that the extended model (6) recovers the model (3) for $\gamma = 0$.

Remark 2. The ensemble's mean velocity (5) follows an Ornstein-Uhlenbeck process for any potential function U . Thanks to the telescopic form of the model (6) and the periodic boundaries we have

$$d\bar{p}(t) = \gamma(u - \bar{p}(t)) dt + \frac{\sigma}{N} \sum_{n=1}^N dW_n(t), \quad t \in [0, \infty).$$

In addition, the ensemble's mean velocity (5) relaxes to u for the deterministic system with $\sigma = 0$.

2.3 Port-Hamiltonian formulation

Next, we rewrite the extended system (6) in matrix form and identify a port-Hamiltonian structure.

Proposition 3. Let $Z(t) = (Q(t), p(t))^T \in \mathbb{R}^{2N}$, $t \in [0, \infty)$. Then the dynamics of the periodic system (6) are given by

$$dZ(t) = (J - R)\nabla H(Z(t)) dt + Su dt + G dW(t), \quad (7)$$

$$Z(0) = z(0) = (\mathfrak{Q}, \mathbf{p})^T \in \mathbb{R}^{2N},$$

with

$$\begin{aligned} J &= \begin{bmatrix} 0 & A \\ -A^T & 0 \end{bmatrix} \in \mathbb{R}^{2N \times 2N}, \\ R &= \begin{bmatrix} 0 & 0 \\ 0 & \beta A^T A + \gamma I \end{bmatrix} \in \mathbb{R}^{2N \times 2N}, \\ A &= \begin{bmatrix} -1 & 1 & & \\ & \ddots & \ddots & \\ & & -1 & 1 \\ 1 & & & -1 \end{bmatrix} \in \mathbb{R}^{N \times N}, \end{aligned} \quad (8)$$

$$S = \begin{pmatrix} 0 \\ \gamma \mathbf{1} \end{pmatrix} \in \mathbb{R}^{2N}, \quad G = \begin{bmatrix} 0 \\ \sigma I \end{bmatrix} \in \mathbb{R}^{2N \times N},$$

$\mathbf{1} = (1, \dots, 1) \in \mathbb{R}^N$ and the Hamiltonian operator $H: \mathbb{R}^{2N} \rightarrow \mathbb{R}$,

$$H(Q, p) = \frac{1}{2} \|p\|^2 + \sum_{n=1}^N U(Q_n), \quad p \in \mathbb{R}^N, \quad Q \in \mathbb{R}^N. \quad (9)$$

The matrix J is skew-symmetric by $N \times N$ block, while R is symmetric positive semi-definite.

Proof. First note that for all $(Q, p)^\top \in \mathbb{R}^{2N}$ we have

$$(\nabla H)(Q, p) = \begin{bmatrix} U'(Q) \\ p \end{bmatrix}, \quad \text{with } U'(Q) = (U'(Q_n))_{n=1}^N.$$

We also have

$$A^\top A = \begin{bmatrix} 2 & -1 & & -1 \\ -1 & 2 & -1 & \\ & \ddots & \ddots & \ddots \\ & & -1 & 2 & -1 \\ -1 & & & -1 & 2 \end{bmatrix} \in \mathbb{R}^{N \times N}.$$

It follows directly from the extended model (6) that

$$\begin{cases} dQ(t) &= Ap(t) dt, \\ dp(t) &= (-A^\top U'(Q(t)) - (\beta A^\top A + \gamma I)p(t)) dt \\ &\quad + \gamma u dt + \sigma dW(t) \end{cases} \quad (10)$$

and therefore

$$dZ(t) = \tilde{B} \nabla H(Z(t)) dt + Su dt + G dW(t)$$

with

$$\tilde{B} := \begin{bmatrix} 0 \\ -A^\top & -\beta A^\top A - \gamma I \end{bmatrix} = J - R \quad \text{and} \quad S = \begin{bmatrix} 0 \\ \gamma I \end{bmatrix}.$$

It is clear that J is skew-symmetric and R is symmetric. Furthermore, it holds for all $(Q, p)^\top \in \mathbb{R}^{2N}$ that

$$(Q^\top, p^\top) R \begin{pmatrix} Q \\ p \end{pmatrix} = \beta \|Ap\|^2 + \gamma \|p\|^2 \in [0, \infty)$$

and therefore R is positive semi-definite.

Remark 4. In the model, the Hamiltonian and the skew-symmetric matrix J represent the conservative part of the system. The velocity terms and the relaxation term to the desired velocity are part of the dissipation matrix R , the input matrix S , and the input control u . Note that the model (3) with $\gamma = 0$ is a stochastic Hamiltonian dissipative system while the extended model (6) with $\gamma > 0$ is a stochastic port-Hamiltonian system with input u .

Remark 5. Using the skew-symmetry of J and the Itô formula, we obtain for the Hamiltonian H given by (9), after simplifications, that

$$\begin{aligned} dH(Z(t)) &= (-\beta \|Ap(t)\|^2 + \gamma \langle p(t), u \mathbf{1} - p(t) \rangle) dt \\ &\quad + \frac{N\sigma^2}{2} dt + \sigma p^\top(t) dW(t). \end{aligned} \quad (11)$$

Note that thanks to the skew symmetry, the Hamiltonian behaviour does not depend on the positions of the agents and the distance-dependent interaction potential U (parameter α).

3. LONG-TIME BEHAVIOUR

We now consider the dynamics of the difference to the desired speed u

$$\tilde{p}_n(t) = p_n(t) - u, \quad t \in [0, \infty), \quad n \in \{1, \dots, N\}, \quad (12)$$

$\tilde{p}(t) = (\tilde{p}_n(t))_{n=1}^N$ and $\tilde{Z}(t) = (Q(t), \tilde{p}(t))^\top$. Note that $\tilde{Z}(t) = Z(t)$ for the initial model (3) for which $u = 0$.

The process \tilde{Z} satisfies

$$d\tilde{Z}(t) = B\tilde{Z}(t) dt + G dW(t), \quad t \in [0, \infty), \quad (13)$$

with

$$B = \begin{bmatrix} 0 & A \\ -\alpha^2 A^\top & -\beta A^\top A - \gamma I \end{bmatrix} \quad \text{and} \quad G = \begin{bmatrix} 0 \\ \sigma I \end{bmatrix}.$$

Furthermore, the Hamiltonian time derivative for the deterministic system with $\sigma = 0$ satisfies

$$dH(\tilde{Z}(t))/dt = -\beta \|\tilde{A}\tilde{p}(t)\|^2 - \gamma \|\tilde{p}(t)\|^2 \leq 0. \quad (14)$$

Remark 6. The uniform equilibrium solution for which $Q_n = L/N$ and $p_n = \frac{1}{N} \sum_{j=1}^N p_j(0)$ for all $n \in \{1, \dots, N\}$ is stable for the deterministic model (3) with $\sigma = 0$ and a quadratic potential (4) for all $\alpha \in (0, \infty)$ and $\beta \in (0, \infty)$.

Remark 7. The uniform equilibrium solution for which $Q_n = L/N$ and $p_n = u$ for all $n \in \{1, \dots, N\}$ is stable for the deterministic model (6) with $\sigma = 0$ and a quadratic potential (4) for all $\alpha \in (0, \infty)$, $\beta \in (0, \infty)$ and $\gamma \in (0, \infty)$.

Indeed, the Hamiltonian H given by (9) is a convex operator which is minimal for the uniform configuration $Q_n^u = L/N$ and $p_n^u = p^u$ for all $n \in \{1, \dots, N\}$, $p^u = \bar{p}(0)$ for the initial model (3) and $p^u = u$ for the extended model (6). Then the decrease of the Hamiltonian with time (14) provides the stability of the deterministic systems.

Interestingly, both the deterministic motion models (3) and (6) with a quadratic potential (4) and $\sigma = 0$ have stable uniform solutions. However, only the extended model (6) with a control input u in a port-Hamiltonian framework remains stable when stochastically perturbed. In the next result we show a weak convergence to a Gaussian distribution. In Proposition 10 we determine the covariance matrix of this stationary distribution and in Corollary 11 we present its limit as the number of agents N tends to infinity.

Remark 8. In Proposition 9 below the spectral analysis of B is extended based on the results given in Ehrhardt et al. (2024). However, we can note beforehand that each block of B is circulant and we have for $\lambda \in \mathbb{C}$

$$|B - \lambda I_{2N}| = |C|, \quad C = \lambda^2 I_N + \lambda(\beta A^\top A + \gamma I_N) + \alpha^2 A^\top A.$$

The matrix $C = \begin{bmatrix} c_0 & c_{N-1} & \dots & c_1 \\ c_1 & c_0 & \dots & c_2 \\ \dots & \dots & \dots & \dots \\ c_{N-1} & c_{N-2} & \dots & c_0 \end{bmatrix}$, with $c_0 = \lambda^2 +$

$\lambda(2\beta + \gamma) + 2\alpha^2$, $c_1 = c_{N-1} = -\lambda\beta - \alpha^2$, and $c_j = 0$ for all $j \in \{2, \dots, N-2\}$, is circulant. Since the determinant of a circulant matrix is given by $|C| = \prod_{j=0}^{N-1} (c_0 + c_{N-1}\omega^j + c_{N-2}\omega^{2j} + \dots + c_1\omega^{(N-1)j})$, where $\omega = e^{2\pi i/N}$, we obtain the characteristic equation of the matrix B as

$$\begin{aligned} &\prod_{j=0}^{N-1} (\lambda^2 + \lambda(2\beta + \gamma) + 2\alpha^2 - (\lambda\beta + \alpha^2)(\omega^j + \omega^{(N-1)j})) \\ &= \prod_{j=0}^{N-1} (\lambda^2 + \lambda(\beta\mu_j + \gamma) + \alpha^2\mu_j) = 0, \end{aligned}$$

where $\mu_j = 2 - \omega^j - \omega^{(N-1)j} = 2 - 2\cos\left(\frac{2\pi j}{N}\right)$. From this we can directly compute the eigenvalues of B leading to (15) in the proof of Proposition 9.

Proposition 9. If $\gamma > 0$ then the process \tilde{Z} converges weakly as $t \rightarrow \infty$ to a Gaussian distribution with mean vector $[L/N \mathbf{1} \ 0]^\top \in \mathbb{R}^{2N}$.

Proof. We first generalise some results of Ehrhardt et al. (2024) to the case $\gamma \neq 0$. In particular, we present the eigenvalue decomposition of the system matrix B . To this end, let $\lambda_{0,1} = 0$, $\lambda_{0,2} = -\gamma$ and for all $j \in \{1, \dots, N-1\}$, $k \in \{1, 2\}$ let $\mu_j = 2 - 2 \cos(\frac{2\pi j}{N}) \in [0, 4]$ and

$$\lambda_{j,k} = \frac{1}{2} \left(-(\beta\mu_j + \gamma) + (-1)^k \sqrt{(\beta\mu_j + \gamma)^2 - 4\alpha^2\mu_j} \right) \in \mathbb{C}. \quad (15)$$

We have $B = \mathcal{W}\Lambda\mathcal{W}^{-1}$, where $\mathcal{W} \in \mathbb{C}^{2N \times 2N}$ is given in (Ehrhardt et al., 2024, Setting 3.1) and $\Lambda \in \mathbb{C}^{2N \times 2N}$ is the diagonal matrix with the vector of eigenvalues

$$[\lambda_{0,1} \ \lambda_{1,1} \ \dots \ \lambda_{N-1,1} \ \lambda_{0,2} \ \lambda_{1,2} \ \dots \ \lambda_{N-1,2}] \in \mathbb{C}^{2N}$$

on its diagonal. To see this note that B only differs from the system matrix B in Ehrhardt et al. (2024) by the term $-\gamma I$ in the lower right block. This entails that the statement of (Ehrhardt et al., 2024, Lemma 3.3) also holds true for B with the only modification that $\lambda_1, \lambda_2 \in \mathbb{C}$ are now the complex roots of $z \mapsto z^2 + (\beta\kappa\tilde{\kappa} + \gamma)z + \alpha^2\kappa\tilde{\kappa}$. From this it follows using the same arguments as in (Ehrhardt et al., 2024, Lemma 3.5) that $B = \mathcal{W}\Lambda\mathcal{W}^{-1}$. Note that $\lambda_{0,1} = 0$ and that all other eigenvalues $\lambda_{j,k}$ have strictly negative real part (in particular, in contrast to the situation in Ehrhardt et al. (2024), we have $\lambda_{0,2} = -\gamma < 0$).

Next define the process $Y(t) = \mathcal{W}^{-1}\tilde{Z}(t)$, $t \in [0, \infty)$. Then Y solves the complex-valued stochastic differential equation $dY(t) = \Lambda Y(t) dt + \mathcal{W}^{-1}G dW(t)$. Note that (Ehrhardt et al., 2024, Lemma 3.5) provides a closed-form representation of \mathcal{W}^{-1} . In particular it follows that the first row of $\mathcal{W}^{-1}G$ is zero (this is due to the fact that the first row of \mathcal{W}^{-1} is given by $u_{0,1}^* = (v_0^* \ 0)$, see (Ehrhardt et al., 2024, Setting 3.1)). This together with the fact that $\lambda_{1,0} = 0$ implies that the first component Y_1 of Y is constant equal to $Y_1(0)$. The remaining diagonal entries of Λ have strictly negative real parts. From this we conclude that the process $(\text{Re}(Y(t)), \text{Im}(Y(t))), t \in [0, \infty)$, is (degenerate) Gaussian and converges weakly as $t \rightarrow \infty$ to its unique invariant distribution. It follows that also $\tilde{Z}(t) = \text{Re}(\tilde{Z}(t)) = \text{Re}(\mathcal{W})\text{Re}(Y(t)) - \text{Im}(\mathcal{W})\text{Im}(Y(t))$, $t \in [0, \infty)$, converges weakly as $t \rightarrow \infty$ to its unique invariant distribution. Since the invariant distribution of Y has a mean vector $(Y_1(0), 0)^\top$, we obtain that the mean vector of the invariant distribution of \tilde{Z} is given by

$$\begin{aligned} \mathcal{W} \begin{pmatrix} Y_1(0) \\ 0 \end{pmatrix} &= Y_1(0)w_{0,1} = (u_{0,1}^* \tilde{Z}(0))w_{0,1} \\ &= \frac{1}{\sqrt{N}} \sum_{k=1}^N \tilde{Z}_k(0) \frac{1}{\sqrt{N}} \begin{pmatrix} \mathbf{1} \\ 0 \end{pmatrix} = \frac{L}{N} \begin{pmatrix} \mathbf{1} \\ 0 \end{pmatrix} \end{aligned}$$

where we used the notation of (Ehrhardt et al., 2024, Setting 3.1) and the fact that $\sum_{k=1}^N \tilde{Z}_k(0) = L$. This concludes the proof.

The covariance matrix Σ of the limiting Gaussian distribution of Proposition 9 necessarily satisfies the matrix Lyapunov equation associated with the system \tilde{Z} (see, e.g.,

(Gardiner, 1985, Section 4.4.6) or (Pavliotis, 2014, Section 3.7)). In our setting this equation is (see (13))

$$B\Sigma + \Sigma B^\top = -GG^\top. \quad (16)$$

In the next steps we will show that (16) uniquely determines Σ and derive its closed-form representation. To do this we write

$$\Sigma = \begin{bmatrix} V_1 & V_2 \\ V_2^\top & V_3 \end{bmatrix} \in \mathbb{R}^{2N \times 2N} \quad (17)$$

for some $V_2 \in \mathbb{R}^{N \times N}$ and symmetric $V_1, V_3 \in \mathbb{R}^{N \times N}$. Then (16) is equivalent to

$$\begin{aligned} AV_2^\top &= -V_2A^\top, \quad AV_3 - \alpha^2V_1A - \beta V_2A^\top A = \gamma V_2 \quad (18) \\ \alpha^2(A^\top V_2 + V_2^\top A) &+ \beta(A^\top AV_3 + V_3A^\top A) + 2\gamma V_3 = \sigma^2 I. \quad (19) \end{aligned}$$

From the symmetry of the system we conclude that the matrices V_1, V_2, V_3 are circulant and that V_2 is also symmetric. In particular, we have that V_3 is determined by a vector $v = (v_0, \dots, v_{N-1})^\top \in \mathbb{R}^N$ via

$$V_3 = \begin{bmatrix} v_0 & v_{N-1} & \dots & v_1 \\ v_1 & v_0 & \dots & v_2 \\ \dots & \dots & \dots & \dots \\ v_{N-1} & v_{N-2} & \dots & v_0 \end{bmatrix} \quad (20)$$

and similarly V_1 and V_2 . Since circulant matrices commute, we see that (19) is equivalent to $\beta A^\top AV_3 + \gamma V_3 = \frac{\sigma^2}{2} I$. Since V_3 is completely determined by v , it suffices to look at the first column of this matrix equation which is $(\beta A^\top A + \gamma I)v = \frac{\sigma^2}{2} e_1$, where $e_1 \in \mathbb{R}^N$ is the first standard unit vector. Since $(\beta A^\top A + \gamma I)$ is circulant, this linear system is equivalent to the convolution equation $w * v = \frac{\sigma^2}{2} e_1$, where $w = (2\beta + \gamma \ -\beta \ 0 \ \dots \ 0 \ -\beta)^\top \in \mathbb{R}^N$ is the first column of $\beta A^\top A + \gamma I$. Next we apply the discrete Fourier transform \mathcal{F}_N to this equation to obtain for each $k \in \{0, 1, \dots, N-1\}$ that $[\mathcal{F}_N(w)](k)[\mathcal{F}_N(v)](k) = \frac{\sigma^2}{2} [\mathcal{F}_N(e_1)](k)$. Using that $[\mathcal{F}_N(w)](k) = 2\beta + \gamma - \beta(e^{-2\pi i k/N} + e^{2\pi i k/N})$ and $[\mathcal{F}_N(e_1)](k) = 1$ and applying the inverse Fourier transform gives

$$\begin{aligned} v_j &= \frac{\sigma^2}{2N} \sum_{k=0}^{N-1} \frac{e^{2\pi i j k/N}}{2\beta + \gamma - \beta(e^{-2\pi i k/N} + e^{2\pi i k/N})} \\ &= \frac{\sigma^2}{2N} \sum_{k=0}^{N-1} \frac{\cos(2\pi j k/N)}{\gamma + 4\beta \sin^2(\pi k/N)}. \end{aligned} \quad (21)$$

This determines V_3 .

Next we use (18) to show that $V_2 = 0$. Note that the fact that V_2 is symmetric and circulant, together with the first equation in (18), ensures that it satisfies $(A + A^\top)V_2 = 0$. Since the kernel of $A + A^\top$ is spanned by $\mathbf{1}$, we conclude that V_2 is a multiple of $\bar{\mathbf{1}}$, where $\bar{\mathbf{1}} \in \mathbb{R}^{N \times N}$ is the matrix consisting only of 1s. Multiplying the second equation in (18) by $\mathbf{1}$ (remember that $\mathbf{1} = (1, \dots, 1)^\top \in \mathbb{R}^N$) implies $\gamma V_2 \mathbf{1} = 0$, which finally gives $V_2 = 0$.

The block V_1 can now be derived from the second equation in (18). Again, due to the cyclicity of V_3 , this equation is equivalent to $V_3 A = \alpha^2 V_1 A$, and so we can read off the solution $V_1 = \frac{1}{\alpha^2} V_3$. Note, however, that A is not regular, but only of rank $N-1$, with $\mathbf{1} \in \mathbb{R}^N$ being the basis of its kernel. From this we conclude that the solution set of $V_1 = \frac{1}{\alpha^2} V_3$ is given by $\{\alpha^{-2}(V_3 + \kappa \bar{\mathbf{1}}) \mid \kappa \in \mathbb{R}\}$. Next, note that for

all $t \in [0, \infty)$ we have that $\sum_{n=1}^N Q_n(t) = L$. This implies that $0 = \mathbf{1}^\top V_1 \mathbf{1} = \alpha^{-2} \mathbf{1}^\top (V_3 + \kappa \mathbf{1}) \mathbf{1} = \alpha^{-2} (N \sum_{j=0}^{N-1} v_j + \kappa N^2)$. This implies that $\kappa = -\frac{1}{N} \sum_{j=0}^{N-1} v_j = -\frac{\sigma^2}{2\gamma N}$. So we have $V_1 = \alpha^{-2} (V_3 - \frac{\sigma^2}{2\gamma N} \mathbf{1})$. We summarise these results in the following proposition.

Proposition 10. Suppose $\gamma > 0$. Then the covariance matrix of the limiting distribution of \tilde{Z} (cf. Proposition 9) is given by (17) with V_3 given by (20) and v by (21), $V_2 = 0$ and $V_1 = \alpha^{-2} (V_3 - \frac{\sigma^2}{2\gamma N} \mathbf{1})$.

Next, we present the limit of the covariance matrix as the number of agents N tends to infinity.

Corollary 11. Suppose $\gamma > 0$ and for all $N \in \{3, 4, \dots\}$, $j \in \{0, 1, \dots, N-1\}$ let v_j^N be given by (21). Then it holds for all $\tilde{N} \in \{3, 4, \dots\}$, $j \in \{0, 1, \dots, \tilde{N}-1\}$ that $(v_j^N)_{N \in \{\tilde{N}, \tilde{N}+1, \dots\}}$ converges to $\frac{\sigma^2 a^j}{2F}$ with $a = 1 + \frac{\gamma}{2\beta} - \frac{F}{2\beta}$ and $F = \sqrt{\gamma^2 + 4\beta\gamma}$.

Proof. Let $a = 1 + \frac{\gamma}{2\beta} - \frac{F}{2\beta}$ and $b = 1 + \frac{\gamma}{2\beta} + \frac{F}{2\beta}$ with $F = \sqrt{\gamma^2 + 4\beta\gamma}$, and observe that $a \in (0, 1)$ and $b > 1$. For all $j \in \mathbb{N}_0$ let $g_j: \{z \in \mathbb{C}: |z| < b\} \rightarrow \mathbb{C}$, $g_j(z) = \frac{\sigma^2 z^j}{2\beta(b-z)}$ and note that g_j is a holomorphic function on $\{z \in \mathbb{C}: |z| < b\}$. Further, let $\Gamma: [0, 1] \rightarrow \mathbb{C}$, $\Gamma(t) = e^{2\pi i t}$. Observe for all $N \in \{3, 4, \dots\}$, $j \in \{0, 1, \dots, N-1\}$ that $v_j \equiv v_j^N$ in (21) is a Riemann sum and that it holds that

$$v_j^N = \frac{1}{N} \sum_{k=1}^N \frac{g_j\left(\Gamma\left(\frac{k}{N}\right)\right) \Gamma\left(\frac{k}{N}\right)}{\Gamma\left(\frac{k}{N}\right) - a}.$$

We thus consider for all $j \in \mathbb{N}_0$ the line integral

$$\frac{1}{2\pi i} \int_{\Gamma} \frac{g_j(z)}{z-a} dz = \int_0^1 \frac{g_j(\Gamma(t)) \Gamma(t)}{\Gamma(t) - a} dt.$$

By Cauchy's integral formula, we have for all $j \in \mathbb{N}_0$ that

$$\frac{1}{2\pi i} \int_{\Gamma} \frac{g_j(z)}{z-a} dz = g_j(a) = \frac{\sigma^2 a^j}{2F}.$$

Therefore, we obtain for all $j \in \mathbb{N}_0$ that

$$\begin{aligned} \lim_{N \rightarrow \infty} \frac{1}{N} \sum_{k=1}^N \frac{g_j\left(\Gamma\left(\frac{k}{N}\right)\right) \Gamma\left(\frac{k}{N}\right)}{\Gamma\left(\frac{k}{N}\right) - a} &= \frac{\sigma^2 a^j}{2F} \\ &= \frac{\sigma^2 \left(1 + \frac{1}{2} \frac{\gamma}{\beta} - \frac{1}{2} \sqrt{\left(\frac{\gamma}{\beta}\right)^2 + 4 \frac{\gamma}{\beta}}\right)^j}{2\beta \sqrt{\left(\frac{\gamma}{\beta}\right)^2 + 4 \frac{\gamma}{\beta}}}. \end{aligned}$$

4. SIMULATION RESULTS

In this section we present simulations of $N = 10$ agents moving according to the dynamics (3) and (6) along a segment of length $L = 501$ with periodic boundaries and $\alpha = \beta = \sigma = 1$. The simulations are performed from a uniform zero velocity initial condition using an Euler-Maruyama scheme with a time step of $dt = 0.001$. The trajectories over the first 500 time units are shown in Fig. 2. The upper panel shows the trajectories for the diverging dynamics (3) with $\gamma = 0$, where the ensemble's mean velocity follows a Brownian motion. The middle and lower panels show the trajectories of the extended port-Hamiltonian model with $\gamma = 0.1$ and $\gamma = 1$, respectively,

where the velocities of the vehicles remain close to the control input velocity $u = 0$.

The simulations can be run in real time on the online platform at: https://www.vzu.uni-wuppertal.de/fileadmin/site/vzu/Simulating_Collective_Motion.html?speed=0.7.

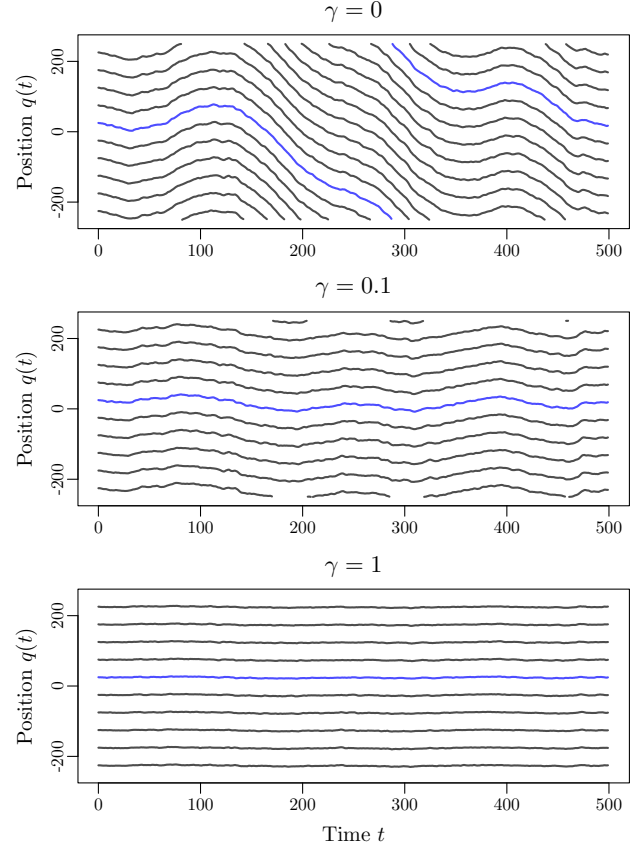


Fig. 2. Trajectories of 10 vehicles along a segment of length $L = 501$ with periodic boundaries with the dynamics (6) with $\gamma = 0$ (the ensemble's mean velocity diverges, upper panel) and with the pHS with $\gamma = 0.1$ and $\gamma = 1$ and the controlled input velocity $u = 0$ (middle and lower panels).

5. CONCLUSION

This study has revisited and analysed a symmetric port-Hamiltonian single-file model in one dimension, emphasising the impact of white noise on its stability. The introduction of a control term within the port-Hamiltonian framework has proven effective in stabilising the dynamics, even in the presence of noise. These findings offer valuable insights for enhancing the control of road traffic flows.

Future research may explore time-dependent control strategies ($u = u(t)$), distance-dependent control ($u = u(Q_n)$) as seen in the model by Rüdiger et al. (2022), agent-specific controls ($u = u_n$), and random controls with uncertainties ($u = U$). These potential extensions provide a rich landscape for further investigation and refinement, contributing to the ongoing development of robust and adaptable models for traffic flow control.

REFERENCES

- Bansal, H., Schulze, P., Abbasi, M.H., Zwart, H., Iapichino, L., Schilders, W.H., and van de Wouw, N. (2021). Port-Hamiltonian formulation of two-phase flow models. *Systems & Control Letters*, 149, 104881.
- Chandler, R.E., Herman, R., and Montroll, E.W. (1958). Traffic dynamics: studies in car following. *Operations Research*, 6(2), 165–184.
- Ciuffo, B., Mattas, K., Makridis, M., Albano, G., Anesiadou, A., He, Y., Josvai, S., Komnos, D., Pataki, M., Vass, S., and Szalay, Z. (2021). Requiem on the positive effects of commercial adaptive cruise control on motorway traffic and recommendations for future automated driving systems. *Transportation Research Part C: Emerging Technologies*, 130, 103305.
- Dai, S. and Koutsoukos, X. (2020). Safety analysis of integrated adaptive cruise and lane keeping control using multi-modal port-Hamiltonian systems. *Nonlinear Analysis: Hybrid Systems*, 35, 100816.
- Ehrhardt, M., Kruse, T., and Tordeux, A. (2024). The collective dynamics of a stochastic port-Hamiltonian self-driven agent model in one dimension. *ESAIM: Mathematical Modelling and Numerical Analysis*.
- Friesen, M., Gottschalk, H., Rüdiger, B., and Tordeux, A. (2021). Spontaneous wave formation in stochastic self-driven particle systems. *SIAM Journal on Applied Mathematics*, 81(3), 853–870.
- Gardiner, C. (1985). *Handbook of Stochastic Methods*, volume 3. Springer Berlin.
- Gasser, I., Siritto, G., and Werner, B. (2004). Bifurcation analysis of a class of ‘car following’ traffic models. *Physica D: Nonlinear Phenomena*, 197(3-4), 222–241.
- Gunter, G., Gloude-mans, D., Stern, R.E., McQuade, S., Bhadani, R., Bunting, M., Delle Monache, M.L., Lysecky, R., Seibold, B., Sprinkle, J., et al. (2020). Are commercially implemented adaptive cruise control systems string stable? *IEEE Transactions on Intelligent Transportation Systems*, 22(11), 6992–7003.
- Jacob, B. and Totzeck, C. (2023). Port-Hamiltonian structure of interacting particle systems and its mean-field limit. *arXiv preprint arXiv:2301.06121*.
- Knorn, S., Donaire, A., Agüero, J.C., and Middleton, R.H. (2014). Scalability of bidirectional vehicle strings with measurement errors. *IFAC Proceedings Volumes*, 47(3), 9171–9176.
- Kometani, E. and Sasaki, T. (1958). On the stability of traffic flow (report-I). *Journal of the Operations Research Society of Japan*, 2(1), 11–26.
- Makridis, M., Mattas, K., Anesiadou, A., and Ciuffo, B. (2021). OpenACC. an open database of car-following experiments to study the properties of commercial ACC systems. *Transportation Research Part C: Emerging Technologies*, 125, 103047.
- Matei, I., Mavridis, C., Baras, J.S., and Zhenirovskyy, M. (2019). Inferring particle interaction physical models and their dynamical properties. In *2019 IEEE 58th Conference on Decision and Control (CDC)*, 4615–4621.
- Orosz, G., Wilson, R., and Stépán, G. (2010). Traffic jams: dynamics and control. *Philosophical Transactions of the Royal Society A: Mathematical, Physical and Engineering Sciences*, 368(1928), 4455–4479.
- Pavliotis, G. (2014). *Stochastic processes and applications: diffusion processes, the Fokker-Planck and Langevin equations*, volume 60 of *Texts in Applied Mathematics*. Springer.
- Pipes, L.A. (1953). An operational analysis of traffic dynamics. *Journal of Applied Physics*, 24(3), 274–281.
- Rashad, R., Califano, F., Schuller, F.P., and Stramigioli, S. (2021a). Port-Hamiltonian modeling of ideal fluid flow: Part I. Foundations and kinetic energy. *Journal of Geometry and Physics*, 164, 104201.
- Rashad, R., Califano, F., Schuller, F.P., and Stramigioli, S. (2021b). Port-Hamiltonian modeling of ideal fluid flow: Part II. Compressible and incompressible flow. *Journal of Geometry and Physics*, 164, 104199.
- Rashad, R., Califano, F., van der Schaft, A., and Stramigioli, S. (2020). Twenty years of distributed port-Hamiltonian systems: a literature review. *IMA Journal of Mathematical Control and Information*, 37(4), 1400–1422.
- Reuschel, A. (1950). Fahrzeugbewegungen in der Kolonne. *Österreichisches Ingenieur Archiv*, 4, 193–215.
- Rüdiger, B., Tordeux, A., and Ugurcan, B. (2022). Stability analysis of a stochastic port-Hamiltonian car-following model. *arXiv preprint arXiv:2212.05139*.
- Sharf, M. and Zelazo, D. (2019). Analysis and synthesis of mimo multi-agent systems using network optimization. *IEEE Transactions on Automatic Control*, 64(11), 4512–4524.
- Tordeux, A., Costeseque, G., Herty, M., and Seyfried, A. (2018). From traffic and pedestrian follow-the-leader models with reaction time to first order convection-diffusion flow models. *SIAM Journal on Applied Mathematics*, 78(1), 63–79.
- Tordeux, A., Roussignol, M., and Lassarre, S. (2012). Linear stability analysis of first-order delayed car-following models on a ring. *Physical Review E*, 86(3), 036207.
- Tordeux, A. and Schadschneider, A. (2016). White and relaxed noises in optimal velocity models for pedestrian flow with stop-and-go waves. *Journal of Physics A: Mathematical and Theoretical*, 49(18), 185101.
- Tordeux, A. and Totzeck, C. (2023). Multi-scale description of pedestrian collective dynamics with port-Hamiltonian systems. *Networks and Heterogeneous Media*, 18(2), 906–929.
- Treiber, M. and Helbing, D. (2009). Hamilton-like statistics in onedimensional driven dissipative many-particle systems. *The European Physical Journal B*, 68, 607–618.
- Treiber, M. and Kesting, A. (2017). The intelligent driver model with stochasticity-new insights into traffic flow oscillations. *Transportation Research Procedia*, 23, 174–187.
- van der Schaft, A. and Jeltsema, D. (2014). Port-Hamiltonian systems theory: An introductory overview. *Foundations and Trends in Systems and Control*, 1(2-3), 173–378.
- Wilson, R. and Ward, J. (2011). Car-following models: Fifty years of linear stability analysis – a mathematical perspective. *Transportation Planning and Technology*, 34(1), 3–18.